PERGAMON

Water Research 37 (2003) 3023–3033

WATER RESEARCH

www.elsevier.com/locate/watres

Kinetic analysis for the removal of a reactive dye from aqueous solution onto hydrotalcite by adsorption

N.K. Lazaridis*, T.D. Karapantsios, D. Georgantas

Division of Chemical Technology, School of Chemistry, Aristotle University, Box 116, Thessaloniki GR-54124, Greece

Received 31 May 2002; accepted 20 February 2003

Abstract

The removal of a reactive color, Cibacron Yellow LS-R, from aqueous solutions by adsorption onto hydrotalcite particles is investigated using batch rate experiments. Measurements are performed at various initial color concentrations, solid loads, pH values and ionic backgrounds (dissolved NaCl). The speed of agitation and the temperature inside the batch adsorber are also varied within a practical range of values. It is shown that the sorption capacity is relatively high for most experimental conditions so hydrotalcite may be considered as a suitable sorbent for this application. The probable mechanism of the process is investigated by a number of homogeneous and heterogeneous reaction kinetic models as well as diffusion kinetic models. It is found that no single kinetic model can fully describe the sorption process at all times. At least three independent rate-controlling mechanisms appear to compete each other and dominate the different stages of sorption.

Keywords: Adsorption; Diffusion; Hydrotalcite; Kinetics; Mass transfer; Reactive dye

1. Introduction

Over the last few decades sorption (as adsorption, biosorption and ion exchange) has gained importance as an effective purification and separation technique used in wastewater treatment, due to the generation or use of some innovative materials/biomaterials [1]. One such promising material is the family of synthetic compounds called hydrotalcites or hydrotalcite-like compounds or layered double hydroxides [2]. The most famous class is Mg–Al hydrotalcites with the general formula $[Mg^{2+}_{1-x}Al^{3+}_{x}(OH)_2]^{x+}[A^{n-}_{x/n}\cdot mH_2O]^{x-}$, where A^{n-} is an n-valent anion and x can have values between 0.2 and 0.33. The interlayer anions and water molecules can be exchanged with other anions, so hydrotalcites are theoretically good anionic exchangers [3].

Dyes are normally present in dyehouse effluent at concentrations of 10–50 mg/L, color being notable at concentrations above 1 mg/L. Dyehouse effluents are complex, containing a wide and often varied range of dyes and a variety of other products, e.g. dispersants, salts, acids, alkalis. The extent to which reactive dyes are lost in exhaust and wash liquors is in the range 20–50% [4]. Reactive dyes are, in general, the most problematic among other dyes, as they tend to pass through conventional treatment systems unaffected. Municipal aerobic treatment systems, dependent on biological activity, were found to be ineffective in the removal of these dyes. Chemical, physical and biological methods have been used for the removal of dye from dye-containing industrial effluents [5–7]. Among them, specific reference must be addressed to flotation that was employed in our lab with particular success [8].

Kinetic analyses [9,10] not only allow estimation of sorption rates but also lead to suitable rate expressions characteristic of possible reaction mechanisms. It must be stressed though that the problem of finding an

*Corresponding author. Tel.: +30-2310-997807; fax: +30-2310-997759.

E-mail address: nlazarid@chem.auth.gr (N.K. Lazaridis).

0043-1354/03/$ - see front matter
doi:10.1016/S0043-1354(03)00121-0

Nomenclature

A	pre-exponential factor (min^{-1})
c	constant
C	bulk solution concentration (mg/L)
C_e	equilibrium bulk solution concentration (mg/L)
D_c, D_p	micropore, macropore diffusivity (cm^2/s)
E	apparent activation energy ($kJ\,mol^{-1}$)
$f(\alpha)$	conversion rate function
$g(\alpha)$	integrated conversion rate function
k, k_2, k_m	rate constants
K_L	constant in Langmuir equation (L^{-1}/g)
n	apparent reaction order
p_n	numerically determined parameters
q	sorption capacity (mg color/g hydrotalcite)
q_e	equilibrium sorption capacity (mg color/g hydrotalcite)
q_m	maximum sorption capacity (mg color/g hydrotalcite)
q_t	instantaneous sorption capacity (mg color/g hydrotalcite)
R	gas constant ($8.3136\,J\,mol^{-1}\,K^{-1}$)
R_p	particle radius (cm)
T	temperature (°C)
t	time (min)

Greek letters

α	degree of conversion
α_L	constant in Langmuir equation (L/mg)
β_2	constant
ε_p	void fraction
Λ	fraction of ultimately adsorbed color
ξ	numerically determined parameter (cm/s)

appropriate conversion function with time is much simpler than establishing a real mechanism for a process. A satisfactory rate equation does not always provide enough information to establish the reaction mechanism but fortunately this is not a requirement for process equipment design. So, the calculated kinetic parameters can be of a great practical value for technological applications since kinetic modeling successfully replaces time- and material-consuming experiments. According to Chen et al. [11], there are four main model representations commonly used for describing adsorption with significant mass transfer resistance: (i) the reaction rate approach (ii) linear driving force expressions for the internal and external mass transport processes (iii) non-linear driving force expressions and (iv) reversible or irreversible adsorption.

Sorption of a sorbate in *liquid* solution by *solid* sorbent particles represents an interesting situation in terms of kinetic analysis since ideas for both constant volume homogeneous reactions and heterogeneous reactions may approximately apply. This is so because under well-mixed conditions, the system is macroscopically homogeneous whereas on a microscopic scale the interaction of the liquid solution with the solid particles constitutes a typical heterogeneous process.

Many studies engaged so far to study sorption phenomena involved analysis of batch experiments where data were sampled at wide time intervals over the entire course of the process. As a result, very fast changing kinetic data characteristic of the phenomena just after the onset of sorption could not be accurately depicted in an adequately short time scale. The aim of this study is to investigate the kinetic mechanism of color sorption on HT particles putting more emphasis on samples collected at short times after the initiation of the process where the major part of the adsorption occurs.

In this paper, we study the suitability of several analytical methods for the kinetic analysis of sorption. In addition to testing some conventional kinetic models, a few alternative solid-state models, successfully employed in the past to the degradation of polymeric systems, are also examined.

2. Kinetic background

To compare measurements from various experiments for a kinetics investigation, it is necessary to introduce a dimensionless degree of conversion. Thus, by normalizing the remaining color concentration, C_t, with respect to some reference value, an index of sorption is defined. Taking advantage of the values of C_t before the onset of sorption, C_0, and for completed sorption, $C_\infty = C_e$, the following degree of conversion is proposed:

$$\alpha = \frac{C_0 - C_t}{C_0 - C_e}. \tag{1}$$

Kinetic studies customary utilize the basic conversion rate equation:

$$\frac{d\alpha}{dt} = k(T) f(\alpha), \tag{2}$$

where $f(\alpha)$ is a conversion-dependent function and $k(T)$ is the reaction rate constant. Sorption has been accepted to follow Arrhenius kinetics [12], which means that the temperature dependence of the rate constant k may be

described by the well-known Arrhenius expression:

$$k(T) = A\exp(-E/RT). \quad (3)$$

An integrated expression of Eq. (2) often appears in literature as

$$g(\alpha) = \int_0^{\alpha} \frac{d\alpha}{f(\alpha)} = k(T)t. \quad (4)$$

Both $f(\alpha)$ and $g(\alpha)$ are functions representative of theoretical models that must be derived with respect to the mechanism of the reaction. There are many proposed methods to calculate kinetic parameters and often the reported values do not depend only on experimental conditions but also on mathematical treatment of data [13]. That is why, we analyzed the measurements of this work by several techniques to increase the calculation confidence.

2.1. Simple homogeneous reactions

Analyses originally developed for isothermal homogeneous reactions were reported to apply also to sorption by postulating a constant system volume [14]. In several earlier sorption experiments where a single deceleratory rate behavior predominated, it was assumed that the conversion function, $f(\alpha)$, could be represented as

$$f(\alpha) = (1-\alpha)^n. \quad (5)$$

Most simple reactions have integer orders, n, between zero and three. For sorption the value of n was customary one or two [31]. In a constant volume system, the time necessary for a given fraction of a limiting reagent to react will depend on the initial composition of the reactants in a manner that is determined by the rate expression for the reaction. This fact is the basis for the development of the *fractional life* method for the analysis of kinetic data [15]. The fractional life approach is most useful as a means of obtaining a preliminary estimate of the reaction order. Moreover, it cannot be used for systems that do not obey nth-order rate expressions.

For constant volume systems, the data of one experimental run or from different runs using the same initial composition, may be utilized to determine the times necessary to achieve different fractional conversions, α. The ratio of these times ($t_{\alpha 1}$ and $t_{\alpha 2}$) is given by

$$\frac{t_{\alpha 1}}{t_{\alpha 2}} = \frac{1/(1-\alpha_1)^{n-1} - 1}{1/(1-\alpha_2)^{n-1} - 1} \quad \text{for } n \neq 1 \quad (6)$$

and

$$\frac{t_{\alpha 1}}{t_{\alpha 2}} = \frac{\ln(1-\alpha_1)}{\ln(1-\alpha_2)} \quad \text{for } n = 1. \quad (7)$$

The value of this ratio is characteristic of the reaction order. Table 1 contains a tabulation of some useful ratios of partial reaction times. By using such ratios based on experimental data, one is able to obtain a quick estimate of the reaction order with minimum effort.

Table 1
Ratios of partial reaction times for constant volume systems

Reaction order, n	0	1	2	3
$t_{0.15}/t_{0.35}$	0.429	0.377	0.328	0.281
$t_{0.15}/t_{0.70}$	0.214	0.135	0.076	0.038
$t_{0.35}/t_{0.70}$	0.500	0.358	0.231	0.135

2.2. Simple heterogeneous reactions

It is generally accepted that solid–liquid reactions can follow a large variety of kinetic equations. In fact, the apparent occurrence of simple-order equations is mainly coincidental [16]. Many authors have derived expressions that reflect the nature of various reaction types. These may be conveniently recognized from experimental data using the *reduced-time plot* method (e.g. [17,18]). In this method, all forms of kinetic expressions are written in the form:

$$g(\alpha) = c\frac{t}{t_{0.50}}, \quad (8)$$

where c is a constant calculated from the actual form of the kinetic expression, and $t_{0.50}$ is the reaction's half-life (time to 50% conversion). Nine most often used $g(a)$ functions and their corresponding c values are given in Table 2 [32].

The selection of the $g(\alpha)$ function is based on the shape of a reduced-time plot which describes best the experimental data. By calculating values of α for several different kinetic equations and plotting them against $t/t_{0.50}$, curves with a characteristic shape are obtained. Theoretical predicted fractions, α, versus $t/t_{0.50}$, for the various reactions of Table 2, can be seen in Fig. 8 against experimental data of this study (more about the comparison later). Although the analytical expressions in Table 2 are so different, the respective theoretical curves look quite similar. In fact, data can be classified into three distinct groups. The first group includes the four homogeneous solid phase diffusion equations, the second group includes the moving phase boundary and first-order decay equations and the third includes the 2D and 3D random nucleation (Avrami–Erofeev) equations. The proximity between some models in Fig. 8 makes it difficult to identify the correct reaction mechanism. It is apparent that differentiation within these groups requires very careful and precise experimental data. Several authors have successfully used the reduced-time plot method to assist in the study of

Table 2
Some common solid-state reaction kinetic equations

Reaction type, g(α)	c-value	Rate-controlling process
$D_1(\alpha) = \alpha^2$	0.2500	Diffusion, 1D
$D_2(\alpha) = (1-\alpha)\ln(1-\alpha) + \alpha$	0.1534	Diffusion, 2D
$D_3(\alpha) = [1-(1-\alpha)^{1/2}]^2$	0.0426	Diffusion, 3D (spherical symmetry)
$D_4(\alpha) = (1-2\alpha/3) - (1-\alpha)^{2/3}$	0.0367	Diffusion, 3D (contracting sphere model)
$R_2(\alpha) = [1-(1-\alpha)^{1/2}]$	0.2929	Moving phase boundary, 2D
$R_3(\alpha) = [1-(1-\alpha)^{1/3}]$	0.2063	Moving phase boundary, 3D
$F_1(\alpha) = \ln(1-\alpha)$	−0.6931	Random nucleation, first-order decay law
$A_2(\alpha) = [-\ln(1-\alpha)]^{1/2}$	0.8326	Random nucleation, 2D
$A_3(\alpha) = [-\ln(1-\alpha)]^{1/3}$	0.8850	Random nucleation, 3D

the thermal decomposition of a variety of polymers (e.g. [19]).

3. Materials and experimental techniques

3.1. Materials

The adsorbent used in this investigation was hydrotalcite SD1520 kindly supplied by Crosfield (now INEOS Silicas). Typical data about this material, denoted hereafter as HT, are: (i) Surface area 100 m^2/g by N_2 BET, (ii) Pore volume 0.5 mL/g by N2 BET, (iii) Volume average pore size 30 nm and (iv) Particle diameter $\sim$8 μm by particle size analysis (Mastersizer, Malvern). The adsorbate was a bifluoro-functional-azo reactive dye, Yellow LS-R (CI R.Y 208), kindly supplied by Cibacron. The average dimensions of the dye, denoted hereafter as CY, are $\sim$35 Å in length and $\sim$20 Å in width, as calculated theoretically by Chemoffice software (CambridgeSoft. com).

3.2. Analytical techniques—determination of dye concentration

The calibration curve for the dye was prepared by recording the adsorbance values for a range of known concentrations of dye solution at the wavelength of maximum adsorbance ($\lambda_{max} = 402$ nm).

3.3. Equilibrium experiments

Equilibrium experiments, to determine the adsorption capacity of hydrotalcite, were conducted using 150 cm^3 suspensions in conical flasks mixed into a reciprocal shaker at a stirring rate of 200 rpm for 24 h.

3.4. Kinetic experiments

The adsorber reactor vessel for the contact time experiments was based on the standard mixing tank configuration with a volume of 2 L [20]. A Heidolph-type RZR 2102 variable-speed motor was used to drive a disc turbine furnished with six 45°-inclined blades. Samples were extracted at selected time intervals using a syringe. The concentration was determined by employing the adsorbance calibration curve and the results were recorded as concentration versus time. The typical conditions for the experiments in this work are: 0.5 g/L solids, 20 mg/L color, 1100 rpm agitation speed, pH = 8 and 20°C. These conditions hold for all the curves displayed below unless differently stated.

4. Results and discussion

The adsorption equilibrium for a 0.5 g/L solids load in the solution is best described by the Langmuir equation. Porter et al. [21] also found that the Langmuir equation performs better when working with sorption of acidic dyes.

$$q_e = \frac{K_L C_e}{1 + \alpha_L C_e}, \tag{9}$$

where the subscript e denotes equilibrium conditions and best-fit values are $K_L = 511$ and $\alpha_L = 5.54$. Most of the sorption experiments of this work are conducted with this particular solids load.

The effect of the agitation speed on the remaining concentration of color in the bulk is examined first. Speeds between 50 and 1100 rpm are tested (graph not shown due to space limitations) and it is found that only above 350 rpm the response curves become insensitive to agitation. For the rest of this work all runs are conducted with a 1100 rpm speed which assures satisfactory homogeneity in the bulk and decouples the sorption analysis from the concentration distribution in the test vessel. However, it must be stressed that external film diffusion is never completely discarded and may appear relatively more significant during the first few minutes of the sorption tests.

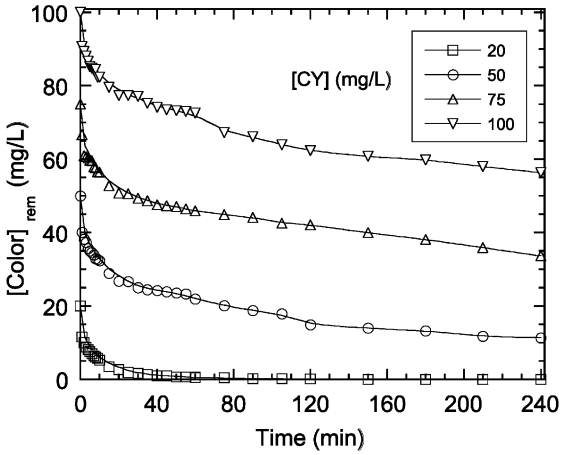

Fig. 1. Remaining color concentration in the bulk versus time for various initial concentrations. [HT] = 0.5 g/L, pH = 8, $T = 20^{\circ}$C and agitation speed 1100 rpm.

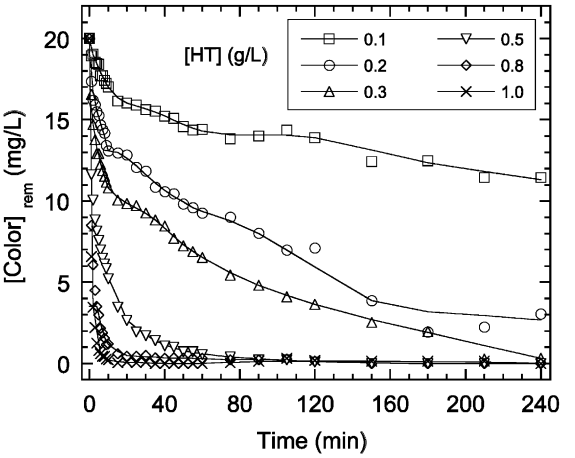

Fig. 2. Remaining color concentration in the bulk versus time for various solid loads. [CY] = 20 mg/L, pH = 8, $T = 20^{\circ}$C and agitation speed 1100 rpm.

The effect of the initial concentration of color in the bulk is depicted in Fig. 1 (0.5 g/L solids). One may discern several gross features in these curves. For all the employed concentrations there is a monotonous decreasing trend with time with the steep descent at the beginning of sorption being succeeded by a more gradual decay. Considering the equilibrium values for the three more concentrated solutions ($C_e^{100} = 47.8$; $C_e^{75} = 29.2$; $C_e^{50} = 4.41$ mg/g; determined experimentally from independent tests) it is seen that even after 4 h, equilibrium is not reached yet. On the contrary, for the 20 mg/L solution the color is completely depleted within 2 h—this curve is inappropriate for kinetic analyses but it is shown for completeness. The qualitative resemblance among curves is considerable despite the different instantaneous driving forces, $C_{bulk} - C_{particle\ surface}$, along runs. This is further manifested by the approximately equal amounts of adsorbed color at $t = 4$ h (42 ± 2 mg/L) for the 50, 75 and 100 mg/L runs. Thus, the overall sorption process is apparently not influenced so much by external mass diffusion, a condition which is desirable for the subsequent kinetic analysis.

A parameter with great significance to the sorption performance is the solids load in the bulk. Fig. 2 displays how solids content affects the sorption of 20 mg/L initial color concentration. Changing the load by one order of magnitude (0.1–1 g/L) has a dramatic effect on both sorption capacity and sorption rate for the employed 4 h of the tests. While for 0.1 mg/L sorption appears clearly incomplete, for loads equal and above 0.3 mg/L, 4 h are adequate for ful removal of the color. Despite the varying adsorption rates, the gross features identified in the curves of Fig. 1 are also present here.

The impact of the presence of other background dissolved ionic substances can give insight regarding the dominant mechanism(s) of sorption. This is also important in evaluating the effectiveness of the treatment. Tests with 1 M NaCl added in the solution are showed in Fig. 3 for several solids load. Evidently, NaCl enhances the adsorption rate but does not seem to influence so much the final sorption capacity as can be seen by comparing the curves for 0.2 mg/L solids in Figs. 2 and 3.

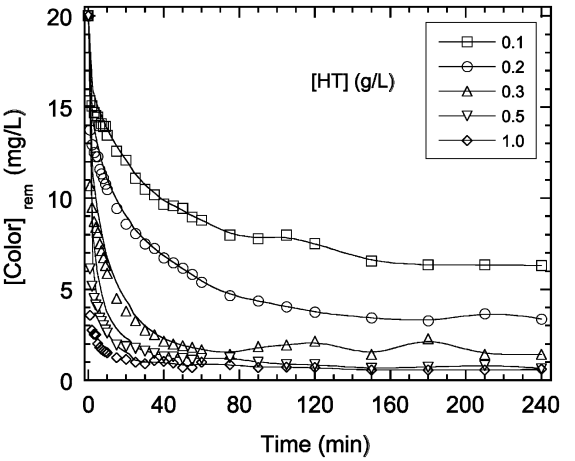

Fig. 3. Effect of 1 M NaCl dissolved in the bulk solution to the remaining color concentration for various solid loads. [CY] = 20 mg/L, pH = 8, $T = 20^{\circ}$C and agitation speed 1100 rpm.

The solution's pH is another important ionic contributor that can influence the process mechanism. Fig. 4 presents a few runs at different pH values. It is clear that color is much faster removed at a low pH environment.

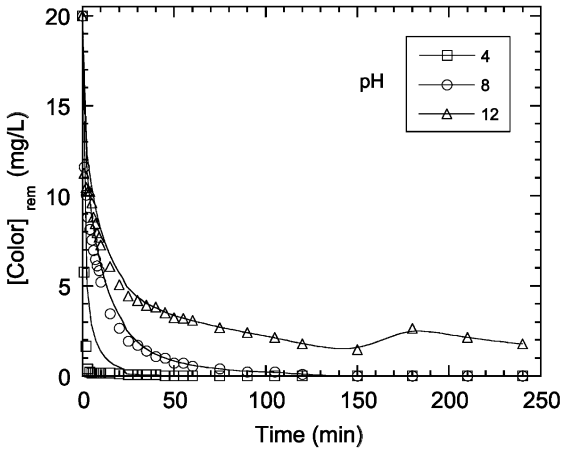

Fig. 4. Effect of pH to the remaining color concentration. [CY] = 20 mg/L, [HT] = 0.5 g/L, $T = 20^{\circ}$C and agitation speed 1100 rpm.

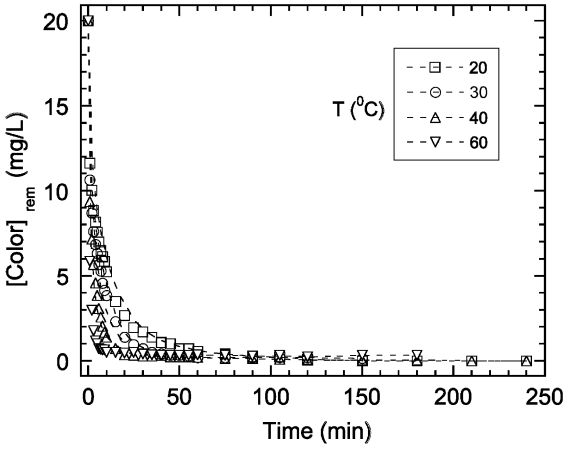

Fig. 5. Effect of temperature to the remaining color concentration. [BY] = 20 mg/L, [HT] = 0.5 g/L, pH = 8 and agitation speed 1100 rpm.

In general, the ionic background is expected to have a stronger effect in chemical than diffusion-controlled sorption processes and it can also alter the equilibrium properties of the sorbate/sorbent system. Which of the two effects prevails and eventually dictates the overall performance is a matter of concern.

Careful inspection of Figs. 2–4 reveals that in some runs (from those that reach equilibrium within 4 h) possible desorption might be witnessed at long times where the color concentration appears to fluctuate or even rise a little. Such desorption phenomena may be attributed to either a reversible reaction or a back diffusion-controlling mechanism both of which show up distinctly only after the cumulative uptake of the sorbate by the sorbent becomes significant. Regarding the first option, reversible reaction models to describe sorption phenomena have been already reported in literature [12]. However, for experiments involving large concentration steps the concentration dependence of diffusivity may give similar results. This is so because although just after the onset of sorption the adsorption rate is faster than the desorption rate, they eventually become comparable at later times. Such counteracting phenomena have been communicated in the past regarding sorption on zeolites [22,23]. In this study, the effect of desorption is limited and so is disregarded from the analysis.

A particularly useful parameter for contrasting kinetic against diffusion models is temperature. Fig. 5 display the adsorption curves obtained at different isothermal conditions. Runs are for 0.5 g/L solids. Apparently, adsorption is accelerated as the temperature of the bulk rises but whether this is due to a chemical reaction or a diffusion-control mechanism requires a quantitative analysis (see below).

5. Mechanism selection

The main issue when searching for an appropriate sorption mechanism is to select a mathematical model that not only fits the data with satisfactory accuracy but also complies with a reasonable sorption mechanism. Thus, in order to identify the correct mechanism several models must be checked for suitability and consistency in a broad range of the system parameters. The model selection criteria proposed by Ho et al. [12] concerning sorption of pollutants in aqueous systems are used as a general guideline. According to this, several reaction-based and diffusion-based tests are performed in order to increase the confidence in simulating our data. Experimental kinetic curves ending with complete depletion of color from the bulk (zero concentration) are excluded from the calculations that follow.

The relatively short duration of the present experiments (4 h) is a first indication that sorption of color is a kinetic rather than a diffusion-controlled process. However, the comparison of elements from Table 1 with calculated fractional life values from the present tests leaves no doubt that simple-order kinetics cannot adequately describe the sorption reaction. Among all homogeneous kinetic equations proposed by Cheung et al. [24], the best fit for the data sets collected in this study is achieved by the so-called modified second-order and the pseudo-second-order rate equations. In integrated form these equations are given as

$$q_t = q_e\left\{1 - \left[\frac{1}{\beta_2 + k_2 t}\right]\right\}, \tag{10}$$

$$\frac{t}{q_t} = \frac{1}{k_m q_m^2} + \frac{1}{q_m} t, \tag{11}$$

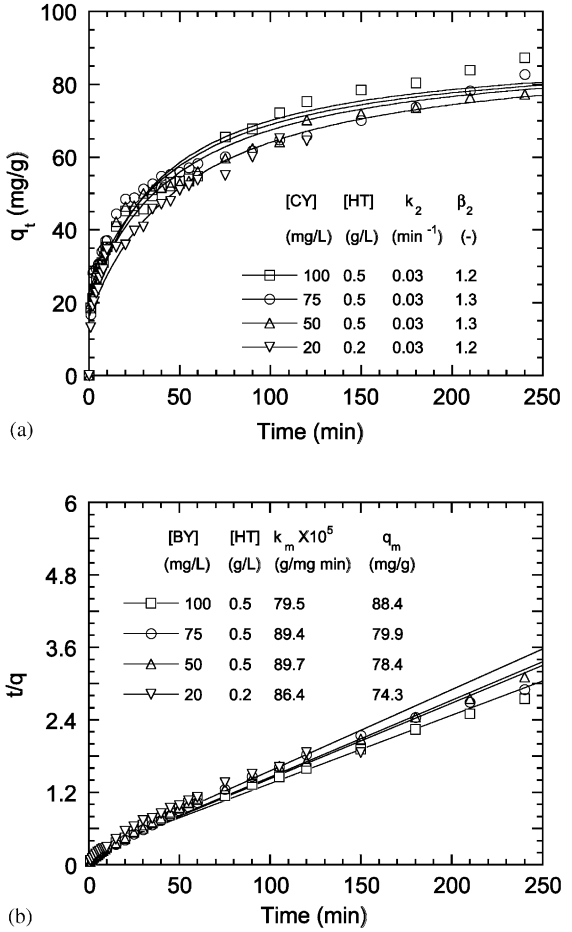

Fig. 6. Comparison of experimental uptake curves against theoretical predictions based on (a) the modified second-order reaction model (Eq. (10)) and (b) the pseudo-second-order reaction model (Eq. (11)).

where q_t is the amount of color adsorbed at any instant ($= (C_0 - C_t)$/solids load), q_e is the amount of color adsorbed at equilibrium ($C_t C_e$) and q_m is a numerically determined parameter which under ideal second-order rate control coincides with q_e. Also, β_2 is the initial unaccomplished surface coverage ($= 1 - q_0/q_e$) and k_2 and k_m are rate constants. The parameter β_2 reflects the pre-absorption of impurities onto the sorbent surface and serves as an extra degree of freedom to make the model more flexible. Figs. 6a and b present the results of fitting Eqs. (10) and (11) to data from selected runs shown in Figs. 1 and 2 employing experimental q_e values determined independently. The inset tables display the numerically best-fit values of the rate parameters. These values are identical or in close proximity among runs—albeit different for the two models—indicating that the modified second-order and the pseudo-second-order models provide a quite suitable description of data for advancing time. Yet, they cannot capture the rapid rate of adsorption during the first minute(s) of the experiments. In this respect, Eq. (10) is advantageous over (11) since it overshoots only the first minute of the process which is however responsible for about 25% of the total adsorption. This acute jump at the beginning of sorption has been considered in the past as indicative of a fast initial external mass transfer step [12]. However, such an extraordinary fast rate of initial color removal may also manifest a fast chemical ion surface attachment.

To shed some light on the above, an *initial rate analysis* is performed to the data in Figs. 1 and 2 [15]. The initial rates (r_0) are taken equal to the slopes of the experimental curves calculated for just the first minute. This analysis is typically valid for a conversion less than 10% which is a condition fulfilled in this case. A log–log plot of r_0 versus C_0 (not shown) provides estimation of the order of the initial reaction. If external mass transfer describes the sorption during this first minute then simple first-order kinetics should be observed. Interestingly, when we performed the analysis to the (constant solids load) curves of Fig. 1a virtually zero-order initial rate is found which practically means that the initial color removal rate is independent of bulk concentration. Furthermore, the initial rates for a constant concentration and variable solids load (Fig. 2) show a clear linear association with the amount of sorbent, which is directly proportional to the external surface area of the sorbent particles. Therefore, it is a reasonable assumption at this stage to assume an initial predominant mechanism of chemical nature rather than external film diffusion. This is further supported by the highly favorable equilibrium isotherm for this sorbate/sorbent system. A possible external phenomenon to conform to this picture may be a surface enhancement associated with a highly energetic heterogeneous sorbent surface [12]. Evidently, more work is needed to elucidate this issue.

Next, the possibility that the sorption data follow a heterogeneous reaction type is examined. Fig. 7 compares sorption data obtained from different initial concentrations with the nine representative kinetic equations of Table 2. Most data lie far off the theoretical curves but closer to the 3D diffusion model. In particular, the higher the initial concentration the closer the particle 3D diffusion model is. It must be mentioned though that the diffusion curves in Fig. 7 are calculated from the typical diffusion equation subjected to a constant bulk concentration boundary condition throughout the sorption experiment.

In order to examine the suitability of intraparticle (pore) diffusion in fitting our data, we plotted the amount of color adsorbed, q_t, versus the square root of time and check for linearity and whether the curve passes through the origin [25]. Fig. 8 presents the results of this test applied to the data of Fig. 1. The inset shows the slope of the lines that represent k_d, the diffusional

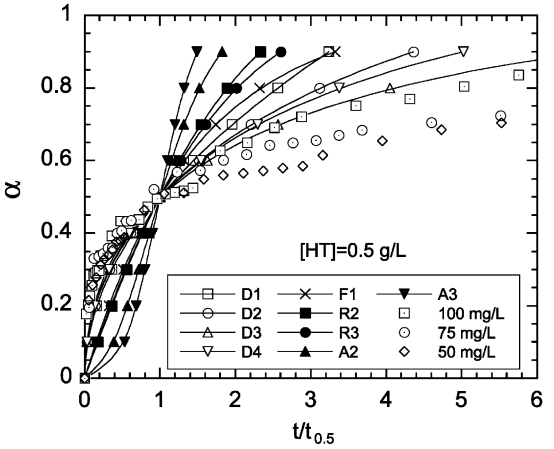

Fig. 7. Reduced-time plot of experimental degree of conversion, α, versus $t/t_{0.5}$ along with theoretical curves calculated for various solid-state reaction equations. Symbols explained in Table 2.

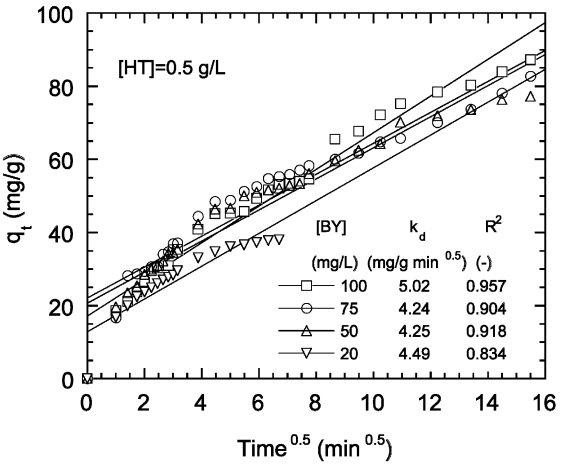

Fig. 8. Plot of sorption capacity versus $t^{0.5}$ to check whether intraparticle (pore) diffusion is a rate-limiting step.

rate constant. Apart from the first minute the fit is fair and this gets better if one considers the possibility of several linear sections in the curves standing for different pore sizes. Besides, comparing the relative sizes of the average pore of H.T. and the dye molecule shows that diffusion may indeed have a chance to play a role in the response of the system. On the other hand, the lines do not pass through the origin and k_d is pretty constant for all runs whereas for intraparticle diffusion a linear variation with the square root of concentration would be expected. The same remarks also hold for the plots (not shown) describing the experiments conducted under various solids loads.

All the above imply two things: (a) there might be a fair chance that a diffusion mechanism controls partly the process, (b) since the goodness of diffusion increases with initial concentration, any diffusion test must take into account the fact that the quantity of color adsorbed during the process is not negligible compared with the initial amount of color. The latter means that the diffusion equation must be solved under a time-dependent boundary condition for the concentration at the surface of the sorbent particle.

The solution of the diffusion equation in spherical coordinates for a time-dependent boundary condition and a concentration-independent diffusivity is given analytically by Ruthven [26]

$$\alpha = 1 - 6\sum_{n=1}^{\infty} \frac{\exp(-\xi p_n^2 t)}{9\Lambda/(1-\Lambda) + (1-\Lambda)p_n^2}, \tag{12}$$

where p_n is given by the non-zero roots of

$$\tan(p_n) = \frac{3p_n}{3 + p_n^2/(1-\Lambda)} \tag{13}$$

and $\Lambda \equiv (C_0 - C_\infty)/C_0$ is the fraction of color ultimately adsorbed by the sorbent.

Eq. (12) can be solved numerically to determine ξ which for the case of particle (also called intracrystalline or micropore) diffusion control equals to D_c/R_c. The same expression is the solution of the diffusion equation for a (macro)pore diffusion control but only in cases where the equilibrium isotherm is linear ($q_e = KC_e$) for the concentration range under investigation. Then ξ equals to $(D_p/R_p^2)/[1 + (1-\varepsilon_p)K/\varepsilon_p]$ where $\varepsilon_p D_p/[1 + (1-\varepsilon_p)K]$ is the effective macropore diffusivity and K is the equilibrium constant. Since the experimental procedure in this work is based on measuring the remaining color concentration in the bulk, Λ is always above 0.5. Only for $\Lambda < 0.1$ the assumption of a constant concentration at the surface of the sorbent is approximately valid and then the diffusion equation can be solved in the conventional way as in Fig. 7. Provided that the employed concentration step in a sorption experiment corresponds to a linear section of the equilibrium isotherm, then the constant K can be replaced by the local slope of the isotherm, dq_e/dC_e. For most runs in this work, e.g. Fig. 1, the equilibrium isotherm is not only linear but also roughly flat ($dq_e/dC_e = 0$) for the employed concentrations.

The non-linear numerical regression to fit data to Eq. (12) is performed by the Levenberg–Marquardt method which gradually shifts the search for the minimum χ^2 from steepest descent to quadratic minimization (Gauss–Newton). Since our interest is chiefly focused in the short time region ($\sqrt{D_{c,p}t/R_{c,p}^2} < 0.2$) where Eq. (12) converges slowly, at least 100 terms are used in the summation to achieve satisfactory accuracy.

Fig. 9 displays the result of fitting Eq. (12) to sorption data obtained with different initial concentrations and

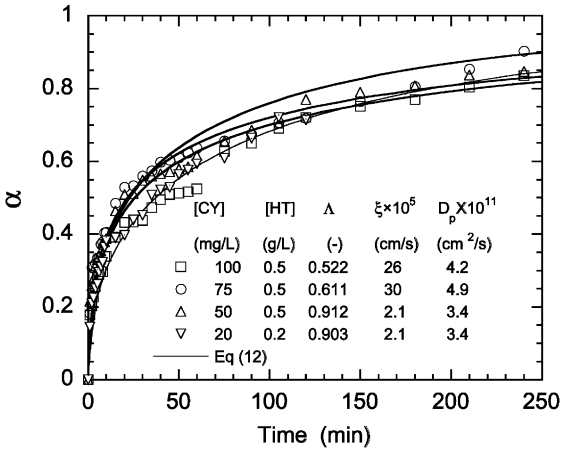

Fig. 9. Experimental degree of conversion, α, against predictions based on the solution of the diffusion equation for a time-dependent bulk concentration (Eq. (12)).

solids load. The inset shows the values of Λ, ξ and the computed values of D_p. It is apparent that this diminishing boundary concentration diffusion model is capable of successfully describing the entire range of data including also the steep concentration gradient of the early removal stage. The ξ values vary about an order of magnitude with a tendency for higher values at higher initial concentrations. If one assumes that diffusion occurs mainly in macropores ($R_p = 4\,\mu m$) then the respective D_p values span from 3.4×10^{-12} to $4.2 \times 10^{-11}\,cm^2/s$. Despite some scatter in the data one may note that the diffusion model performs better for the lower solids load and color concentration; since then mass transport slows down. The scatter is partly ascribed to experimental noise, which is appreciable at least for the first 60 min of the experiments. To assess the significance of this noise a derivative time series analysis is performed where $d\alpha/dt$ is plotted against t and then a Hanning low-pass filter is applied to flatten out the

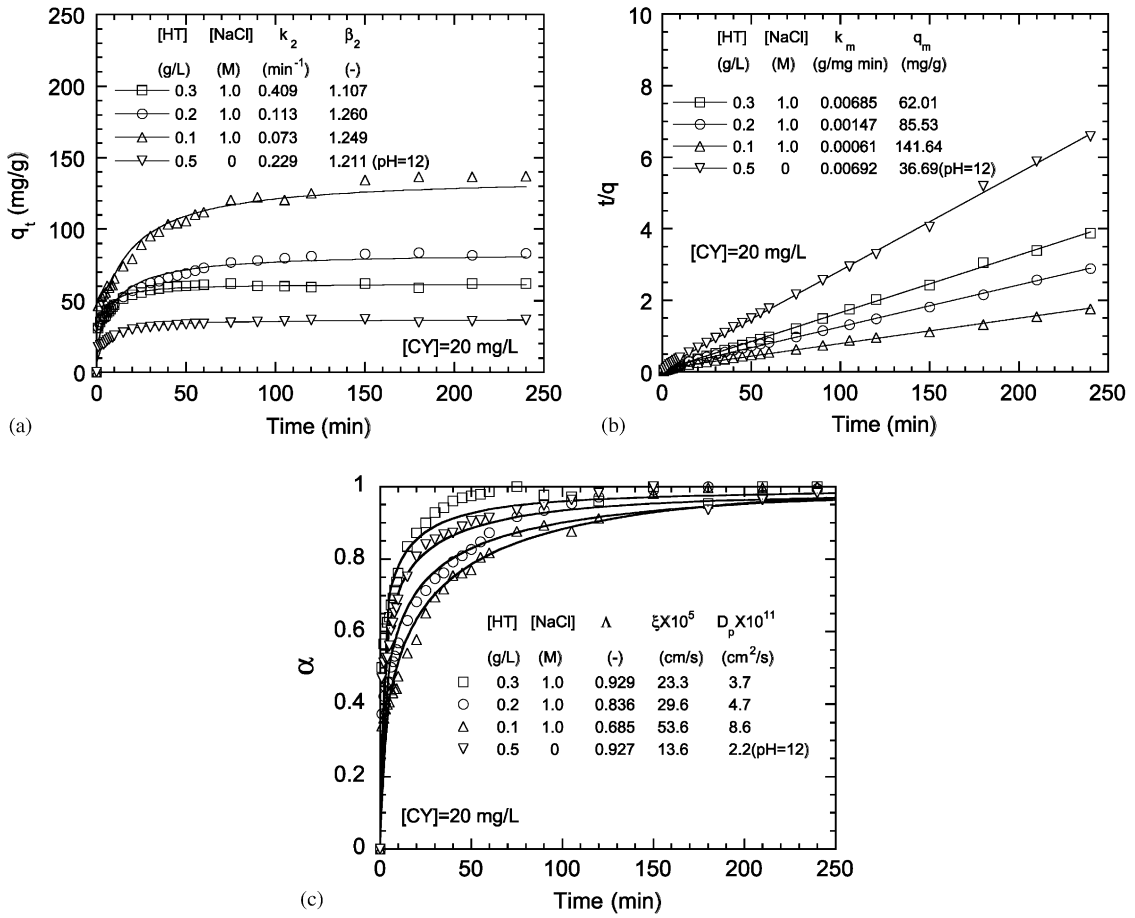

Fig. 10. Application of the theoretical models in (a) Eq. (10), (b) Eq. (11) and (c) Eq. (12) to describe experimental data obtained with various solid loads after adding 1 M NaCl to the bulk solution or adjusting its pH to 12.

signal undulations until $d\alpha/dt$ versus α becomes a reasonably smooth curve [27]. Next, the integrated smoothed signal $\alpha(t)$ is processed as before and resulted in D_p values between 7×10^{-12} and 1.5×10^{-11} cm^2/s.

Next, the above models—Eqs. (10)–(12)—are applied to experiments performed with an added ionic background to the color solution, Figs. 3 and 4. Only runs where the adsorption reached equilibrium within 4 h are treated. The results are presented in Figs. 10a–c where insets include the computed rate parameters. Fig. 10a and b show the best fit of Eqs. (10) and (11) to the data, respectively, whereas Fig. 10c presents the effectiveness of Eq. (12) in this fit. On the whole, it seems that the two second-order kinetic control models describe better the measurements; markedly better than when without ionic background (Fig. 6). As in Fig. 6, the reaction rates calculated by the two second-order models differ by approximately an order of magnitude but they exhibit the same trend when changing the solids load. With the finite diffusion model, not only the fit is poorer but there is also no clear trend in ξ or D_p when the solids content varies. Once more, it appears that this model behaves better for the smaller solids load when transport phenomena are less rapid. The structure of HT (double layer) suggests the presence of two kinds of anion retention sites: sites within the interlayer corresponding to the structural anion exchange capacity (AEC) of the material and adsorption onto external surfaces [28]. The nature of these retention sites lends further support to the notion of a reaction kinetic control model.

Sestak and Berggren [29] suggested that solid-state reactions are activated processes, for which an activation energy may be calculated from the exponential character of $k(T)$ in Eq. (3). Plotting the rate of the reaction against the reciprocal temperature gives a reasonable straight line, the gradient of which is $-E/R$. Ho et al. [12] argues that if an Arrhenius plot is made for k_d, then for a diffusion mechanism to dominate E must be less than 25–30 kJ/mol. This is because the temperature dependence of the pore diffusivity is relatively weak. However, the equilibrium constant, K, which appears in the denominator of the effective macropore diffusivity varies strongly with temperature and this may be misinterpreted as a kinetic sorption scheme.

In the Arrhenius plots (not shown) the correlation is slightly better for the pseudo-second-order reaction ($R^2 = 0.98$) than for diffusion ($R^2 = 0.96$). The respective activation energies calculated from these plots are 58.5 kJ/mol for the pseudo-second-order reaction and 14.8 kJ/mol for the diffusion. So, the experiments conducted at various temperatures do not provide firm evidence in favor of either the kinetic or the diffusion-control mechanism. In view of all the above, one may be tempted to argue that sorption of color is more correctly described by more than one sorption models as is also the practice with the sorption of metal ions, e.g. [30].

6. Conclusions

The present measurements show that the adsorption rate of color onto HT particles is particularly sensitive to solid load, pH and ionic strength of the solution but almost insensitive to initial bulk color concentration. The temperature dependence of sorption rate is somewhat within the usual range of values for both reaction and diffusion kinetic control. Moreover, the important role of agitation speed in decoupling the color–particle interaction from the concentration distribution in the adsorber is displayed. Evidence is provided that the sorption of color on HT particles is a complex process that cannot be adequately described by a single kinetic model throughout the whole process. The present results indicate that the rate-controlling mechanism may vary during the course of the sorption process and at least three mechanisms appear to be capable of effectively competing each other at different stages. These are an *external surface enhancement* or *film diffusion* which dominates the very beginning of the process, a *reaction* which governs the subsequent (and largest) part of the process and finally a *diffusion* which shows up competitively only in occasions where the experimental conditions drastically slow down the transport rates. The favorable uptake capacity and rate of HT particles to the examined color ions demonstrates potential for removing color pollutants from aqueous waste streams. More data under a broader range of experimental conditions are required before conclusive statements can be made.

References

[1] Mc Kay G. Use of adsobents for the removal of pollutants from waste waters. Boca Raton, FL: CRC Press, 1996.
[2] Sato T, Wakabayashi T, Shimada M. Adsorption of various anions by magnesium aluminium oxide. Ind. Eng. Chem. Prod. Res. Dev. 1986;25:89–92.
[3] Bellotto M, Rebours B, Clause O, Lynch J, Bazin D, Elkaïm E. Hydrotalcite decomposion mechanism: a clue to the structure and reactivity of spinel-like mixed oxides. J Phys Chem 1996;100:8535–42.
[4] Laing IG. The impact of effluent regulations on the dyeing industry. Rev. Prog. Coloration 1991;21:56–71.
[5] Delée W, O'Neil C, Hawkes FR, Pihneiro HM. Anaerobic treatment of textile effluents: a review. J. Chem. Technol. Biotechnol. 1998;73:323–35.
[6] Skelly K. Water recycling. Rev. Prog. Coloration 2000; 30:21–34.
[7] Robinson T, MucMullan G, Marchant R, Nigam P. Remediation of dyes in textile effluent: a critical review on current treatment technologies with a proposed alternative. Bioresource Technol 2001;77:247–55.

[8] Mavros P, Daniilidou AC, Lazaridis NK, Stergiou L. Colour removal from aqueous solutions. Part I. Flotation. Environ Technol 1994;15:601–16.
[9] Tien C. Adsorption calculations and modeling. Boston: Butterworth-Heinemann, 1994.
[10] Yiacoumi S, Tien C. Kinetics of metal ion adsorption from aqueous solutions. Boston: Kluwer Academic Publishers, 1995.
[11] Chen B, Hui CW, McKay G. Film-pore modeling and contact time optimization for the adsorption of dyestuffs on pith. Chem Eng J 2001;84:77–94.
[12] Ho YS, Ng JCY, McKay G. Kinetics of pollutants sorption by biosorbents: review. Separation Purification Meth 2000;29(2):189–232.
[13] Smith JM. Chemical engineering kinetics, 3rd ed. Singapore: McGraw-Hill, 1981. p. 37–92; 636–45.
[14] Sparks DL. Kinetics of soil chemical processes.. London: Academic Press, 1989.
[15] Hill CG. An introduction to chemical engineering kinetics and reactor design. New York: Wiley, 1977. p. 24–166.
[16] Froment GF, Bischoff KB. Chemical reactor analysis and design. New York: Wiley, 1979. p. 3–47; 76–130; 141–9.
[17] Ozawa T. Kinetic analysis of derivative curves in thermal analysis. J. Therm Anal 1970;2:301–24.
[18] Rozycki C, Maciejewski M. Method of the selection of the g(a) function based on the reduced-time plot. Thermochim Acta 1987;122:339–54.
[19] Day M, Cooney JD, Wiles DM. A kinetic study of the thermal decomposition of poly(aryl–ether–ether–ketone) PEEK in nitrogen. Polym Eng Sci 1989;29:19–22.
[20] Harnby N, Edwards MF, Nienow AW. Mixing in the process industries, 2nd ed. London: Butterworth-Heinemann, 1992.
[21] Porter JF, McKay G, Choy KH. The prediction of sorption from a binary mixture of acidic dyes using single-and mixed-isotherm variants of the ideal adsorbed solute theory. Chem Eng Sci 1999;54:5863–85.
[22] Kondis FK, Dranoff JS. Kinetics of isothermal sorption of ethane on 4A molecular sieve pellets. Ind Eng Chem Process Des Dev 1971;10(1):108–14.
[23] Satterfield CN, Frabeti AJ. Sorption and diffusion of gaseous hydrocarbons in synthetic mordenite. AIChE J 1967;13(4):731–8.
[24] Cheung CW, Porter JF, McKay G. Sorption kinetic analysis for the removal of cadmium ions from effluents using bone char. Water Res 2001;35(3):605–12.
[25] Milićevic B, McGregor R. Zur thermodynamisch-phänomenologischen beschreibung der färbevorgänge III. Dimensioanalyse der hydrodynamischen effekte. Helvetica Chim Acta 1966;49(7):2098–107.
[26] Ruthven DM. Principles of adsorption and adsorption processes. New York: Wiley, 1984.
[27] Bendat JS, Piersol AG. Random data: analysis and measurement procedures. New York: Wiley, 1986.
[28] Châtelet L, Bottero JY, Yvon J, Bouchelaghem A. Competition between monovalent and divalent anions for calcined and uncalcined hydrotalcite: anion exchange and sorption site. Colloids Surf A: Physicochem Eng Aspects 1996;111:167–75.
[29] Sestak J, Berggren G. Study of the kinetics of the mechanism of solid-state reactions at increasing temperatures. Thermochim. Acta 1971;3:1–12.
[30] Smith EH. Uptake of heavy metals in batch systems by a recycled iron-bearing material. Water Res 1996;30(10):2424–34.
[31] Ho YS, McKay G. Sorption of dye from aqueous solution by peat. Chem Eng J 1998;70(2):115–24.
[32] Brown ME, Dollimore D, Galwey AK. Thermochemistry of decomposition of manganese (11) oxalate dihydrate. Thermochim Acta 1997;21(1):103–10.